

Interpreting Black Hole X-Ray Spectra

Paolo Coppi

Department of Astronomy, Yale University, P.O. Box 208101, New Haven, CT 06520-8101

Abstract. I review the main theoretical conclusions from high-energy spectral observations of Galactic Black Hole Candidate systems. With an eye towards future missions, I show how the ability to reach such conclusions depends critically on the type of spectral coverage one has available. Perhaps the most important factor in determining how well a set of observations constrains theoretical models is the range of energies that can be observed in a simultaneous manner, the wider the better. High spectral resolution observations over a narrow energy band, e.g., as provided by Chandra and eventually ASTRO E-2, are potentially extremely interesting but not as useful as one might first think without an understanding of the underlying broad-band continuum. A snapshot, time-integrated spectrum that has very wide energy coverage, however, is still not sufficient to break all the current model degeneracies. The tightest model constraints instead come from combining spectral with timing information. The RXTE satellite excelled in this regard, enabling unprecedented spectral variability studies on both short and long timescales by virtue of its large collection area, broad energy response, and flexible scheduling. Future instruments, or combinations of instruments, must strive for a similar balance of timing and broad-band spectral capabilities if they are to prove as effective as RXTE.

INTRODUCTION

The last ten or so years have seen significant progress in understanding the physical processes and emission mechanisms at work in galactic black hole binary systems. Although the tenor of the theoretical discussion has improved during this time, e.g., we now think that magnetic fields are responsible for accretion disk viscosity and outflows and we are starting to explicitly calculate their effects on a computer (see contribution by Meier, this proceedings), the basic theoretical concepts we invoke to understand black hole binary systems, e.g., the existence of an accretion disk itself and the production of X-ray continuum by thermal Comptonization, are largely the same as when they were first introduced in the 1970s. It is also still true that we cannot explain from first principles the complex phenomenology we see in an object like GRS 1915. What has changed significantly, however, is our ability to observationally constrain our theoretical thinking. This has come about for two main reasons.

First, the quasi-continuous presence of X-ray instruments in space, in particular of wide field monitors like the ASM, allowed us to significantly increase the sample size of known systems. (Most galactic binaries are short-lived transients and only a few are active at any given time). The subsequent monitoring of these system, both at X-ray/gamma-ray energies and at radio to optical wavelengths, has given us a much fairer sample of what is typical behavior and what is not. Not surprisingly, our best-studied prototypical object, Cyg X-1, turns out not

to be so typical, while a comparison of accreting black hole systems with neutron star ones (also detected by the same X-ray instruments and searches) shows the overall phenomenology to be much more similar than we first thought, e.g., both systems produce relativistic jets, indicating a likely common origin for the behavior.

Second, and the main topic of this contribution, the combination of satellites like Ginga, CGRO, RXTE, and BeppoSax allowed us to obtain for the first time very broad band, high quality X-ray and gamma-ray spectra of these systems, e.g., see the compilation by A. Zdziarski of simultaneous Cyg X-1 spectra (Fig. 1) that spans the range $\sim 0.5 - 5$ MeV. Earlier, narrower band observations either missed crucial spectral features such as the high energy turnover in a Comptonization spectrum due to the finite temperature of the scattering electrons or were over such a small energy range (e.g., 2-10 keV and often with low energy resolution) that the observed spectrum was well fit by a simple power law. Being scale free, power law spectra do not tell much about the underlying physics, witness the large number of mechanisms agile theorists can come up with to produce such spectra. It is the deviation from power law behavior, the most extreme example perhaps being a narrow atomic line, that we can use to set a scale and often gives us the tightest constraints on the physical conditions in a source, e.g., on characteristic temperatures or velocity. Here, I will focus on what we have learned from the continuum spectra of black hole binary systems rather than features such as relativistic iron lines since these are covered elsewhere

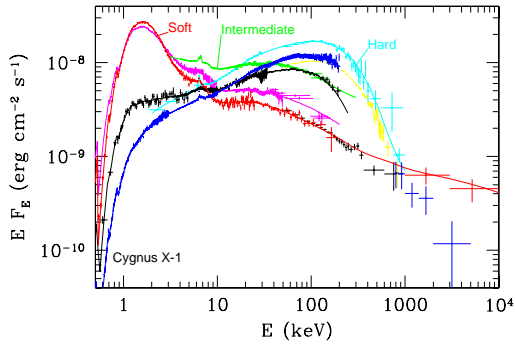


FIGURE 1. Compilation by A. Zdziarski of simultaneous, broad-band Cygnus X-1 spectra for different states obtained by using various combinations of the GINGA, RXTE, BeppoSax, OSSE, and Comptel instruments. The errors in the $\sim 3\text{--}20$ keV range are often dominated by instrument systematics and are often at the few percent level or less. Model fits are made using the EQPAIR hybrid thermal/non-thermal XSPEC emission model [1].

(e.g., the contribution of Reynolds) and the continuum is in some sense more fundamental: it usually contains most of the source luminosity and without a good understanding of it, it is often impossible to compute accurate line diagnostics.

The remainder of the contribution is organized as follows. Because future X-ray and gamma-ray experiments must confront again the difficult tradeoff between cost and energy coverage, in the next section I review the model degeneracies that arise with insufficient coverage. I note that several of the very approximate (e.g., power law) models used for narrower band spectra no longer work well for broad band observations that cover a range of scales. I then summarize some of the main results from recent broad band observations, e.g., by RXTE and BeppoSax, which have successfully broken some of these degeneracies. I conclude by demonstrating that if one is limited to time and spatially averaged spectra, some significant model degeneracies can still remain – even if one does have broad energy coverage. Timing observations with reasonable energy coverage and resolution can break several of these.

To maximize science return, a future mission or set of missions should thus strive to achieve a good balance of timing and broad-band spectroscopic capabilities, as RXTE did. RXTE’s large collection area and scheduling flexibility has enabled us to start to probe the variability of these broad-band spectra, both on short (millisecond) and long (month-year) timescales, allowing us to study the causal connections between spectral states and different emission components and to probe the microphysics on its smallest scales.

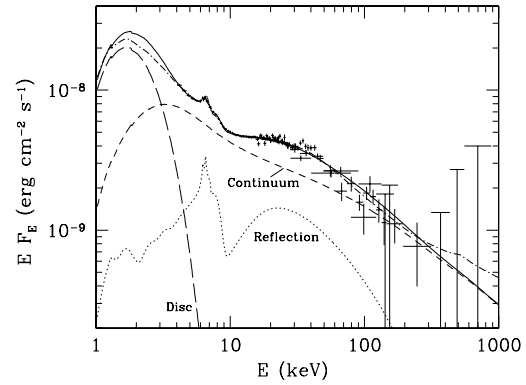


FIGURE 2. Typical ingredients which are required to fit high-quality, broad-band spectrum available for some black hole binaries. The data is from the 1996 soft state spectrum of Cyg X-1 (see [2]), while the model curves are computed using the EQPAIR XSPEC model. The continuum emission in this case is Compton upscattering is by a hybrid, thermal/non-thermal distribution.

THE NEED FOR STRICTLY SIMULTANEOUS, BROAD BAND SPECTRA

As noted, spectra that are not broad band can be often fit by several models or by the same model but with quite different allowed parameter values. In order to understand why these degeneracies can arise, it is useful to run through as a function of energy the main emission components that appear in a typical black hole binary spectrum (e.g., see Fig. 2) and see what information is gained or lost by choosing to observe them or not.

At the lowest energies ($\sim 0.1 - 3$ keV), the spectrum is usually dominated by a black-body like spectrum, thought to be optically thick emission from the accretion disk. This portion of the spectrum is interesting to observe and understand because it contains important information about the radial emission profile of the accretion disk. In particular, since dissipation (and thus the characteristic temperature of disk emission) increases in the standard accretion disk model with decreasing disk radius, the peak energy of the spectrum can tell us about location of the inner edge of the optically thick accretion disk (assuming it truncates sharply at some radius), which is useful for constraining global changes in source geometry with luminosity. Note that in general, one must be quite careful in drawing inferences from the observed seed photon spectrum, e.g., it may be heavily absorbed by intervening matter or Comptonized by electrons in the corona or a boundary layer that is not included in a calculation such as [3]. Determining if this is the case, e.g., if intrinsic absorption exists, requires good data and a good model for the high energy spectrum.

Knowledge of the low-energy spectrum is very important for another reason, however. Photons in this part of the spectrum are usually taken to be the “seed photons” which are Compton upscattered by hot electrons to produce the remainder of the continuum high energy spectrum. The exact nature of the seed photons, e.g., whether they are coronal emission reprocessed by ambient matter or synchrotron/cyclotron photons from coronal electrons (especially non-thermal ones), and their characteristic energy can influence significantly the predicted Comptonization spectrum. For example, given a constant electron heating rate, constant seed photon luminosity, and constant electron scattering optical depth, the predicted Comptonization spectrum softens as the seed photon energy decreases. Also, if the angular distribution of the seed photons is not isotropic, e.g., if the seed photons are reprocessed and emitted by the disk (so no seed photons travel towards the disk), then the spectra of the first few Compton scatterings will reflect this anisotropy, introducing (viewing angle dependent) “anisotropy breaks” in the Comptonized spectrum just above the seed photon peak ([4]). When combined with information about the high energy spectrum, e.g., its luminosity, knowledge of the seed photon distribution can again tell us about source geometry (e.g., the covering fraction of the reprocessing matter, [4]) or mean magnetic field strength ([5]) in the corona.

Moving to higher energies ($\sim 3 - 15$ keV), one encounters several more features. Probably the most well-known now is the reflection spectrum, with its fluorescent iron line/feature at $\sim 6 - 7$ keV and absorption edge at ~ 10 keV (e.g., see Fig. 4, where only the reflection continuum is shown). The iron feature has received considerable attention because its shape is potentially a good probe of the space time geometry near the black hole. Unfortunately, most of the constraints come from the broad red wing of the feature (produced by gravitationally redshifted emission from matter near the innermost orbit), which typically requires a rather accurate determination of the underlying continuum. Without a good broad band spectrum and accompanying continuum model, this is frankly impossible (for examples of difficulties, see [6], [7]). In my own experience using relatively low signal-to-noise RXTE PCA data for Cygnus X-1 (see [8]), it was possible to obtain equally good fits using a line plus a disk black body plus power law continuum model as when using line plus a Comptonized black body model continuum. The inferred line parameters, however, were completely different (and not sensible for the disk black body plus power law continuum model.) Why did this happen? First, the disk black body spectrum was not that well-constrained because of the PCA’s ~ 3 low-energy cutoff. Second, even though Comptonization is supposed to produce a power law, near the seed photon energy it does *not*, especially

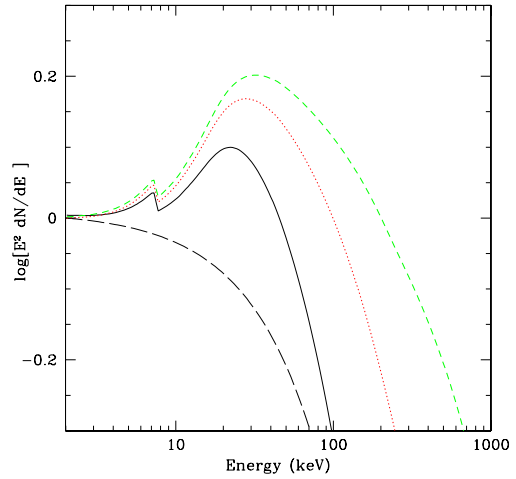


FIGURE 3. Effect on the reflection spectrum due to variation of the maximum energy of the incident source spectrum. The *solid*, *dotted*, and *short-dashed* lines respectively show three PEXRIV XSPEC models (exponentially truncated powerlaw with reflection off partially ionized matter [9]) with the same incident power law index $\Gamma = 2$, reflection fraction $R = 1$, ionization parameter $\xi = 0$ (i.e., neutral matter) but varying truncation energy $E_{cut} = 100, 300$, and 900 keV. The *long-dashed* spectrum shows the incident spectrum for the $E_{cut} = 100$ keV model.

at the error levels that RXTE is capable of. Besides the possible anisotropy break discussed above, distortions in the Comptonization spectrum appear when the scattering electron temperature becomes high. In this case, the energy change of a photon in one scattering is large ($\Delta\epsilon/\epsilon \sim 4kT_e/m_e c^2$), and the first few orders of Compton scattering are still visible in the total Comptonization spectrum ([1], even if there is no anisotropy problem). Constraints on power law deviations in this energy range can thus turn into strong constraints on the maximum allowed temperature of the Comptonizing electrons, and this is one of the key arguments in favor of a non-thermal origin for the power law tail in soft state sources that can extend well-beyond 500 keV (e.g., [2]). (To produce an unbroken power law to such high energies by thermal Comptonization, the electron temperature must be high, but one does not then see the expected low-energy scattering features. This is a good example of low and high energy observations interacting synergistically.)

Another possible complication in extracting the red wing of the line is that high quality data (i.e., broad enough so that all the standard components are well-constrained) sometimes indicates the presence of an extra Comptonization component or more generally, a “soft excess” at these energies (e.g., [7], [10]). Note that the intensity and shape of the iron line can be used to place constraints on possible hot Comptonizing components

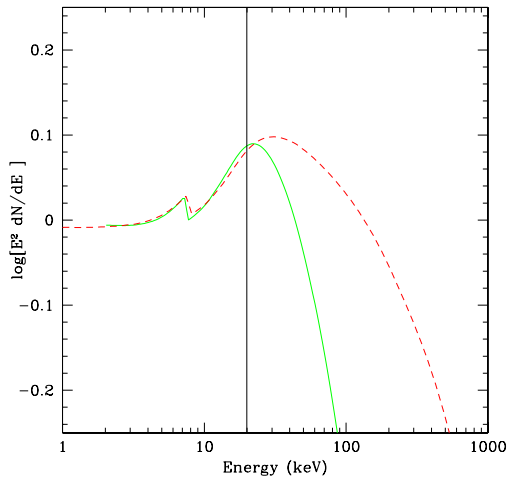


FIGURE 4. Comparison between two PEXRIV models in XSPEC. The *solid* curve shows a model with power law index $\Gamma = 2$, truncation energy $E_{cut} = 100$ keV, reflection fraction $R = 1$, and ionization parameter $\xi = 0$. The *dotted* curve shows a model with the same power law index but now with $R = 0.5$, $E_{cut} = 900$ keV, and $\xi = 100$. The *vertical, solid* line shows the typical energy ($\sim 20 - 30$ keV) where the sensitivities of the PCA and HEXTE instruments on RXTE cross. (HEXTE is better at high energies; PCA is better at low ones.) The reflection fraction and ionization parameters can be traded off against the truncation energy to produce essentially indistinguishable spectra in the PCA energy range.

that intercept the line radiation (since the scattered line would be very Doppler broadened).

This preceding discussion has ignored yet another uncertainty, the shape and intensity of the reflection continuum ([11] [9]) which can be very significant above ~ 10 keV, typically peaking at $\sim 30 - 40$ keV. The continuum is produced when hard photons encounter dense, cold ambient matter and eventually backscatter their way to the observer, losing energy in the process. The main factor governing the strength of the reflection component is, of course, $R = \Omega/2\pi$, the covering fraction of the continuum by the cold matter. As illustrated in Fig. 3 and 4, however, the shape of the incident high energy spectrum, in particular its cutoff energy, is also a critical parameter, as is the ionization parameter for the ambient parameter low energies. By trading off the amount of reflection (R) versus the number of incoming hard photons and tweaking the ionization parameter, it is possible to produce spectral models that have essentially the same low energy spectra but rather different parameters, high energy spectra, and total bolometric luminosities (see Fig. 4) – a serious degeneracy that plagues all observations of hard sources that are restricted to a low energy range. The overall uncertainty concerning reflection is not due just to the tradeoff of reflection fraction vs. high energy

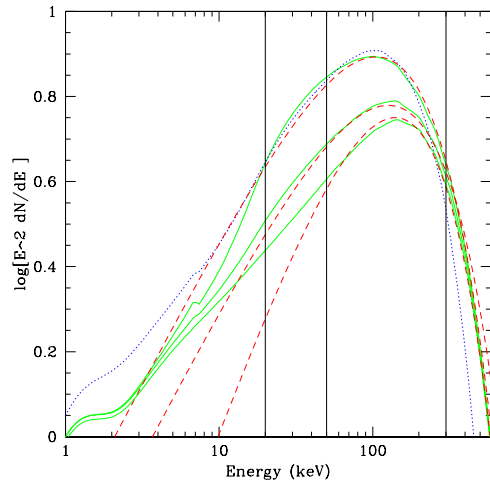


FIGURE 5. The three *heavy solid* lines show EQPAIR thermal Comptonization models with electron temperature $kT_e = 85$ keV, optical depth $\tau_T = 1.29$, and reflection fraction $R = 1.0, 0.26, 0$ from top to bottom respectively. The $R = 0.26$ case is the Rev. 11 model used in [14] to fit RXTE/INTEGRAL data for Cyg X-1. The *solid, vertical* lines at 20 keV, 50 keV, and 300 keV denote respectively the typical transition energy between the PCA and HEXTE instruments on RXTE, the minimum energy of the OSSE instrument on CGRO, and the maximum energy being considered for some next generation hard X-ray satellites. The *dashed* lines show three exponentially truncated powerlaw models chosen to match the EQPAIR models to within 15% in the 50-300 keV energy range. The *dotted* line is another EQPAIR model, but with quite different parameters ($kT_e = 68$ keV, $R = 0.4$, $\tau_T = 1.8$). Note the large divergence between models at low energies despite the good agreement at high energies.

cutoff but also to the tradeoff between reflection fraction vs. ionization parameter that is possible when observing at low energies over a sufficiently restricted band, e.g., see [12]. Note that if one can observe to sufficiently high energies, Klein-Nishina effects always cause the reflection spectrum to break at high energies. In this case it is possible to constrain even completely ionized reflectors that at low energies simply reproduce the incident spectrum, e.g., see [13].

Since future hard X-ray missions may or may not have low-energy detection capabilities on board, it is instructive to ask what happens if one has high energy observations that are not accompanied by good, strictly simultaneous low energy observations, as sometimes happened during the initial days of CGRO. In Fig. 5, we take a baseline model for Cyg X-1 in the hard state [14] and produce two new models by increasing and decreasing the reflection fraction. We then eyeball fit the model spectra being 50-300 keV (the rough range over which the OSSE instrument had good statistics in a moderate length observation) using an exponentially trun-

cated power law, a popular phenomenological model in this energy range. As can be seen, relatively good fits can be made for all reflection fractions using a model that has no reflection included. Also, associating (incorrectly) the peak energy of the observed 50-300 keV spectrum with the temperature of the Comptonizing electrons, one might conclude, for example, that the temperature drops by a factor ~ 2 between the bottom and top spectra. Since the truncated power law is just a phenomenological model (which fails miserably at low energies), one might not be that concerned. More worrisome, however, is the relatively good fit to the $R = 1$ spectrum (down to $\sim 7\text{keV}$) using an $R = 0.4$ (a factor two lower) Comptonization/reflection model that has a lower temperature but higher scattering optical depth for the electrons. Without low energy observations, the model could still be ruled out since it cuts off too sharply at the highest energies, but this requires a detector that can deliver good statistics and systematics above 300 keV. Again, the way to pin down reflection and the considerable uncertainties associated with it is by obtaining a very broad band spectrum.

Fig. 5 also demonstrates another degeneracy that plagued observations, particularly in the early days. Once one gets away from the first few orders of Compton scattering, the slope of the Comptonization spectrum is determined largely by the parameter $y \propto \tau^2 \times kT_e$. An observation that cannot detect the peak of the Comptonization spectrum (which occurs at energy $\sim 3kT_e$, where T_e is the electron temperature) thus cannot measure the electron temperature and thus cannot distinguish between Comptonization by a cold, optically thick plasma versus that by a hot, optically thin plasma – an important distinction if one is trying to ascertain the origin of the hot electrons. An uncertainty in temperature or high energy spectral cutoff, of course, also leads to an uncertainty in the source bolometric luminosity, and the confusing situation that the so-called “low” hard state of Cygnus X-1 (based on 2-10 keV observations) actually has a total luminosity within a factor \sim two in the “high” soft state. Again, having a good handle on bolometric luminosity is a basic requirement for good physical models.

Moving to higher energies still, one might wonder where it is worth stopping. If cost were no issue, the ideal detector would have good sensitivity well beyond 511 keV. Sensitivity to such energies, say ~ 600 keV, is enough to cover adequately most of the cutoffs seen in hard state galactic sources (where it is important for issues such as reflection) and enough to cross an important energy scale, the electron rest mass energy. This energy scale is important for three reasons. First, if bulk motion effects are not important (likely in non-jetted galactic sources), then a photon above this energy interacts with electrons of any energy in the Klein-Nishina limit, where the Compton interaction is significantly reduced. Sec-

ond, photons above this scale have enough energy to pair produce on more abundant lower energy photons (and they should since several galactic sources have moderately high “compactnesses,” i.e., significant pair production opacities above energy $\epsilon m_e c^2$.) Third, the gamma-ray radiation from annihilating electron-positron pairs comes out at $\sim m_e c^2$. In other words, new physical processes kick in and the standard process, Compton scattering, changes. The naive expectation therefore is that the black hole binary spectrum will show some kind of break at energies near 500 keV. To the extent that it does not, as seems the case in several soft state binary sources (e.g., [15],[2], [10]) one then has constraints on quantities like the size and location of the gamma-ray emission region and the importance of electron-positron pairs. At least for currently published models (e.g., [16]), the lack of a break at this energy also causes problems for models which attempt to explain the tail using bulk Comptonization models. (Pair production and pair plasma effects which also become important at such energies might save the models, but this is not clear yet.) Broad band observations cause another potential problem for these models since, as discussed, they allow a good determination of the reflection fraction in the soft state. It seems to be large, ~ 1 [2], which is not expected in the bulk Comptonization model since the fast moving electrons reside in a small region near the black hole, in which case most of their emission should escape to the observer unless the disk is very flared. We note the issue of reflection, which is weaker but still detected in good broad band observations of hard state sources, is also a potential problem for models which attribute most of the observed X-ray emission to emission from power law electrons in a jet, e.g., [17], rather than thermal electrons in a disk corona.

In ideal world, X-ray and gamma-ray observations would be coordinated with ground-based observations at radio, infrared, and optical wavelengths. As is now clear, the phenomenon of black hole binaries is not just an X-ray one, but it manifests itself at many wavelengths, as is the case for Active Galactic Nuclei. Some of these wavelengths, either because of instrumental advantages or because they are the natural energy scale, are better suited for observing certain aspects of the phenomenon. For example, high resolution radio observations have been able to demonstrate the presence of outflows in black hole binaries, some of which appear to be relativistic jets. The correlation between X-ray emission and radio outflows in the hard state is particularly interesting and has opened up a new dimension to the black hole binary problem. (See the contribution by Corbel, these proceedings). Coordinated optical/infrared observations which can track the state of the outer accretion disk and trigger an X-ray observing campaign *before* an X-ray outburst starts have also proven to be very useful, enabling one to unambiguously catch the rapid transition from a low, hard state to

a high, soft state, e.g., [18].

If it is not already clear, one further ingredient is required to make maximal use of broad band observations: sophisticated and accurate fitting models. Because they span (by definition) a large range of energy scales, broad band observations break most models that rely on asymptotic approximations, e.g., most of the Comptonization models in XSPEC (that often only work for electron temperature $kT_e \ll m_e c^2$ and in practice cannot handle temperatures as low as 50 keV). It is also worth remembering that while a power law can be a good first order description for the photon spectrum or electron energy distribution produced by, say, Compton scattering, it is only that, an approximate description – and one that is often not accurate enough to match the requirements of data with 1% errors. Incorrect conclusions, such as the inference of “new” emission components, can and have occurred if overly simple models are used. It should not be a surprise then that as detector collection area and energy coverage improve, one is finding more and more that the standard phenomenological models (such as a power law plus a multi-color disk blackbody) fail entirely to describe the observations. Given the possible complexity of black hole binary spectra that we just have explored, and because such do not have a sound physical basis, one should be very wary of extrapolating too much from the parameters obtained from phenomenological models fits. For a discussion of the shortcomings that even some of the currently more sophisticated (less phenomenological) fitting models have, see [19].

SOME CONCLUSIONS FROM BROAD BAND X-RAY/GAMMA-RAY OBSERVATIONS

Here, I give a brief (and inevitably incomplete and biased) overview of what we have learned from recent broad band observations using considerations of the type just discussed.

First, broad band observations have allowed us to nail down the bolometric luminosity of the source. In terms of total luminosity, the “low” hard state really is still lower in luminosity, but particularly in Cyg X-1, the luminosity in the persistent hard state can actually be quite comparable to that in the soft state, i.e., the transitions in Cyg X-1 are not like those in other non-persistent binaries. The state transitions in Cyg X-1 are also different in that they do not show the “hysteresis” behavior seen in other binaries, where the transition to the soft state occurs at a different luminosity from the transition back to the hard state, e.g., see [20], and the contributions by Tomsick and Smith. This hysteresis behavior, which is also clearly seen in at least one binary with a low magnetic field neu-

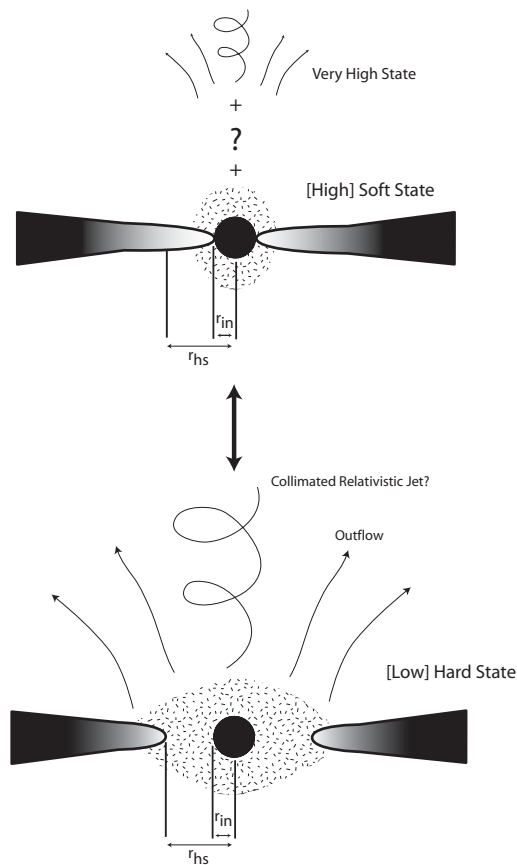


FIGURE 6. Schematic depiction of the source geometries and components currently invoked to explain the various emission states of black hole binaries (see text).

tron star (Aql X-1, [20], [21]), tells us we are missing an important ingredient in our picture for state transitions, i.e., the instantaneous accretion rate is not the only relevant parameter, and that state transitions in neutron stars are presumably not a phenomenon related to the neutron star surface. I note that RXTE’s ability to monitor a source every few hours for an extended period of time was crucial in tracking the hysteresis behavior since the hard to soft transition is very fast (hours).

The broadband observations of the low hard state are well-fit by a Comptonization spectrum and show a cut-off starting at energies $\sim 100 - 300$. This conclusively breaks the spectral degeneracy between cool, optically thick plasmas and hot, optically thin ones in favor of the hot optically thin ones. With the continuum cutoff in hand, we can then robustly probe the behavior of the reflection component, e.g., as a function of state. In Cyg X-1, at least, reflection in the hard state is low with reflection fraction $R \sim 0.2$, but the characteristic reflection “bump” at 30 keV is detected and well-fit by a standard, not heavily ionized reflection component (e.g., see

[8] [14]). It is interesting to note that during the hard state, month-long observing campaign analyzed in [8], Cyg X-1 was remarkably stable in its spectral fit parameters, as long as one considered integration times longer than ~ 1000 sec. (On shorter timescales, flares can be seen and the spectrum clearly varies.) The recent INTEGRAL/RXTE observations by [14] give essentially the same best fit parameters, implying that the basic (average, see discussion below) physical parameters underlying the hard state might be very stable indeed.

A schematic depiction for how the source geometry changes with state is shown in Fig. 6 (see [22], [23], [24]). Heuristically at least, we can explain the observed state behavior by postulating that in the soft state, the inner edge of the optically thick accretion disk reaches down to the marginally stable orbit, while in the hard state, it does not, leaving a “hole” that is perhaps filled by a hot corona. A new piece of information that has been added recently is the correlation with radio emission that suggests an outflow is present in the hard state, disappears in the high, soft state, and perhaps reappears in the ultra-high state. As noted above, the fact that reflection is observed during the hard state puts geometric constraints on a pure jet model explanation for the X-ray emission that are not completely obviously satisfied. While the putative Comptonizing corona could represent the “base” of the jet and, indeed, the fact that it is outflowing at mildly relativistic speeds may naturally explain the observed reflection fraction [25], it seems more likely that correlated radio (“jet”) emission comes from significantly further down the jet, i.e., far away from the disk. A more complete discussion of the implications of the detected reflection component, including an apparent correlation between spectral index and the reflector covering fraction R as well as the “pivoting” behavior of hard state spectrum, can be found in [26]. (Note that the discussion would be impossible without good broadband spectra.)

A non-thermal tail extending past 500 keV is clearly detected in several sources during their soft, high state. Although it is not energetically very significant, the tail indicates a new, likely non-thermal component that is not included in transition models like [23] where the enhanced electron cooling rate during the low state implies a lower electron temperature. As discussed above, because it crosses the $\sim m_e c^2$ energy scale and no strong pair annihilation feature is observed, the power law places constraints on the source compactness (assuming the observed gamma-rays and X-rays are cospatial and not strongly beamed) and causes problems for currently published bulk Comptonization models. “Hybrid” models, where the electron energy distribution has an extended non-thermal tail (not unexpected but currently not well-understood), can instead fit the data well [2]. In general, although there has been much

discussion about the consequences of electron-positron pairs in binaries, there is as yet no conclusive evidence that they are playing an important role in the spectral behavior observed. A hard tail has also been detected in the hard state of Cygnus X-1 (by COMPTEL, [27]), indicating the possible presence of non-thermal electrons in that state too. (The tail could be the direct result of acceleration processes or possibly the decay of π_0 s produced by hot protons in the accretion flow, see introduction in [27].) Unfortunately, the COMPTEL spectrum is integrated over a very long time and the tail is weak. Significantly better sensitivity above 400 keV than was available with CGRO (OSSE and COMPTEL) will be required to probe the temporal evolution of this tail and its connection with the rest of the spectrum.

The standard power law plus multi-color disk black body phenomenological models can fail badly during certain source states, e.g., see [28] for XTE J1550, with the power law component having a higher amplitude than the multi-color disk blackbody component (impossible if the powerlaw is produced by Comptonization of the blackbody) and the blackbody having an impossibly small inferred inner radius. A good fit can be obtained in many of these cases by replacing the blackbody and power law components by a blackbody that is Comptonized by a moderate temperature, optically thick medium, in which case the innermost radius of the seed multi-color blackbody remains stable with reasonable values, e.g., see discussion in [29]. While the physical origin is not completely clear yet, the physics of the accretion disk is again more complicated and diverse than previously thought.

MODEL DEGENERACIES REMAINING IN TIME-AVERAGED, SPATIALLY-AVERAGED SPECTRA

Although we have extolled the virtues of broad band spectra, it is worth noting that they do not address all degeneracies. The model phase space that Nature currently seems to be favoring for black hole binaries is one where anisotropy effects such as spectral breaks are not readily apparent, and the scattering optical depths in a possible corona seem to be moderate (~ 1). The net effect of this is that a broad-band model like EQPAIR [1], which models only one spatial emission zone and thus does a terrible job of radiation transfer, seems to work surprisingly well. In particular, when the total optical depth of a Comptonizing corona is low, seed photons are free to walk around the corona and sample different spatial regions, for example, that may have different temperatures. Since we cannot resolve the X-ray source spatially, the net result is that we see a total spectrum that is charac-

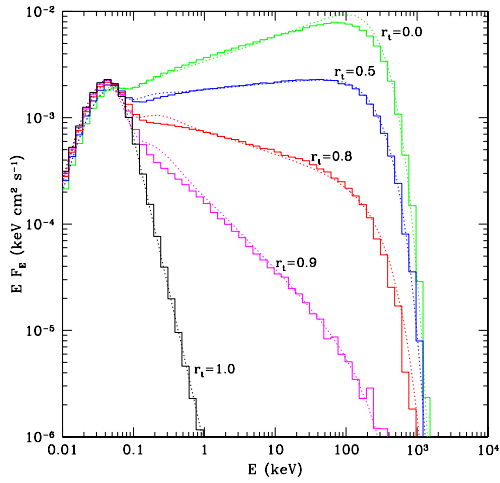


FIGURE 7. Thermal Comptonization spectrum produced by a spatially inhomogeneous source with a hot core of electrons with temperature $kT_{e,hot} = 100$ keV out to a transition radius $r_t \times R_{source}$ that is surrounded by a cool atmosphere of electrons with temperature $kT_{e,cool} = 10$ keV. The *histograms* show exact Monte Carlo calculations for varying transition radii, while the *dotted* lines show fits using the one zone (one temperature, homogeneous source) Comptonization EQPAIR code. The total Thomson optical depth of the source is $\tau_T = 1$. When the optical depth is moderate and photons can scatter back and forth between the hot and cold zones, i.e., the case considered here, the inhomogeneous emergent spectrum is very close to that from a homogeneous source.

terized by spatial averages over quantities like the mean source temperature. As a concrete example, if we have a source that has a hot core surrounded by a cool outer atmosphere, the Comptonization we see is *not* necessarily best described as the sum of a high temperature Comptonization spectrum and a low temperature one. Rather for the case shown in Fig. 7 (where photons start at the center of hot core/cool atmosphere structure), the upscattered spectrum is reasonably described by a *one* temperature Comptonization spectrum, where the relevant temperature is the average temperature seen by the photon as it scatters its way out of the source. To help further the case that all that really matters in predicting the emergent spectrum is the mean number of scatterings a photon undergoes and the mean energy change per scattering, we show in Fig. 8, the Comptonization spectrum produced by a spatially uniform, bi-Maxwellian (two temperature) electron distribution. The spectrum is not the sum of the high and low temperature spectra, but rather is quite close to a one temperature Comptonization spectrum where the inferred electron temperature is roughly the average of the two temperatures. In general, the exact energy distribution of the electrons does not matter as long as the mean electron energy is low and individual photons scat-

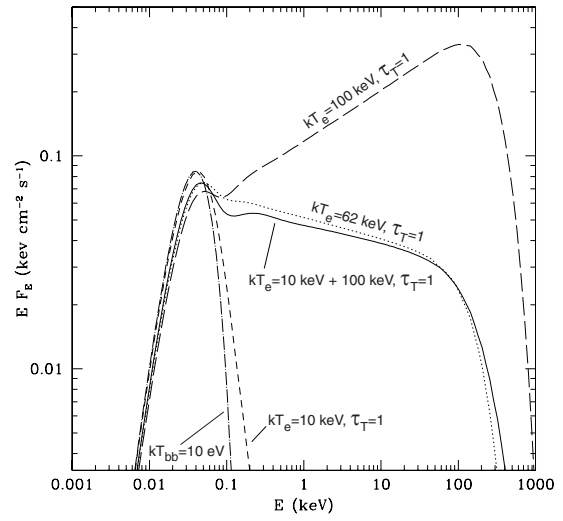


FIGURE 8. The *solid* curve shows the Comptonization spectrum produced by a source uniformly filled by electrons having a bi-Maxwellian (two temperature, 10 keV + 100 keV) electron distribution. The *short-dashed* and *long-dashed* curves show the Comptonization spectra produced when the electron distribution is thermal, with a single temperature of 10 and 100 keV respectively. The *dotted* line shows the Comptonization spectrum produced by a single temperature electron distribution with a temperature (62 keV) close to the average of the bi-Maxwellian temperatures.

ter multiple times to form the observed spectrum, e.g., [1].

As a last example of the effect of spatial inhomogeneities, we change in Fig. 9 the density of the source as a function of radius. As noted in [30], the spectrum after the first Compton scattering can again be fit well by a standard, one temperature, homogeneous Comptonization. This is good news for modelers who may be able to continue to use simple models, but bad news if we wish to use spectra to probe spatial inhomogeneities. For an optically thin source, the information is still there (if one looks in detail at the spectra), but it is very washed by the spatial averaging process of photons traveling throughout the source.

Current data also seem to indicate that pair production effects may not be as important as once speculated. In this case, and especially for low optical depth cases where photons do not spend much time inside the source, this means Compton corona responds relatively quickly and “linearly” to changes in electron and photon injection such as changes in the electron heating rate or the soft photon injection rate. In Fig. 10, we show the practical implications of this using a one-zone time-dependent Comptonization model where the electron heating rate varies up and down randomly each source light-crossing time. The instantaneous emergent spectrum at any given time is not well-fit by a standard Comp-

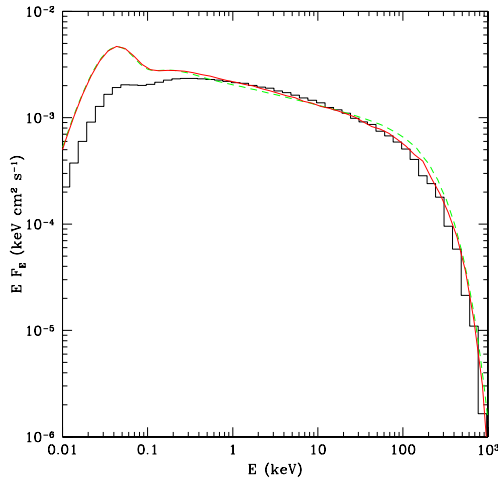


FIGURE 9. The *histogram* shows the Comptonization spectrum produced by an inhomogeneous source where the electron temperature throughout the source is constant ($kT_e = 100$ keV) but the electron density varies as a power law of index $n = 1$ with distance from the center of the source, i.e., $n_e(r) \propto r^{-n}$, with a normalization chosen to produce a total Thomson optical depth of unity as measured radially from the center of the source. The *solid curve* shows the same calculation, except computed for constant electron density, i.e., $n = 0$. For comparison, the *dashed* spectrum shows the one-zone EQPAIR Comptonization spectrum with parameters $kT_e = 100$ keV and $\tau_T = 0.5$. As noted in [30], the resulting spectra are very similar if one only considers the parts of the spectra ($E > 1$ keV) due to photons that have upscattered several times.

tonization spectrum. However, if one instead considers the time-averaged emergent Comptonization spectrum, this *is* indeed quite close to a standard, one-temperature spectrum (that one obtains by using the time-averaged electron heating rate). In other words, again we may expect spectral modelers to have good success using models that might otherwise appear overly simple, but the averaging, this time in time, again wipes out most of the details of the temporal inhomogeneities, i.e., flares. (Note that unlike the case of an AGN, the typical integration time of hundreds to thousands of seconds needed to obtain good broad band statistics corresponds to many dynamical times in the case of a stellar mass black system.)

To summarize, then, temporally and spatially averaged spectra are highly degenerate because only averaged quantities matter and a variety of temporal and spatial source variations can lead to similar averages. The model parameters we derive in fitting such spectra should thus be taken with the appropriate grain of salt; they tell us something about the global properties of the source not the small-scale, short-timescale details. In the case of stellar mass black holes, RXTE has been able to start to crack some of these degeneracies through its fast tim-

ing capabilities which allow it to say something about the profiles individual flares (e.g., [32]) or the proximity of the reflecting matter to the source of the incident spectrum (e.g., [33], [34]). (See also [30] for a more general discussion.) A key reason why RXTE is arguably done better than previous timing missions is that it was able to obtain good timing statistics *over a significant range of energies*. In general, the greater the range of energies, the greater the lever arm one has over models. (Conversely, a huge light bucket with very poor energy resolution or coverage will not be of as much use as one might first think.) A future mission should therefore strive for a good balance of timing and broad-band spectral capabilities.

ACKNOWLEDGMENTS

I thank my collaborators and colleagues Marek Gierlinski, Tom Maccarone, Greg Madejski, Mike Nowak, Juri Poutanen, and Andrzej Zdziarski for many valuable discussions on some of the ideas presented here (as well as help with some of the figures). I thank the organizers for an excellent workshop and for their infinite patience in waiting for this contribution.

REFERENCES

1. Coppi, P. S., “The Physics of Hybrid Thermal/Non-Thermal Plasmas,” in *ASP Conf. Ser. 161: High Energy Processes in Accreting Black Holes*, 1999, p. 375.
2. Gierliński, M., Zdziarski, A. A., Poutanen, J., Coppi, P. S., Ebisawa, K., and Johnson, W. N., *MNRAS*, **309**, 496 (1999).
3. Shimura, T., and Takahara, F., *ApJ*, **445**, 780 (1995).
4. Haardt, F., and Maraschi, L., *ApJ*, **413**, 507 (1993).
5. Wardziński, G., and Zdziarski, A. A., *MNRAS*, **325**, 963 (2001).
6. Reynolds, C. S., and Nowak, M. A., *Phys.Rep.*, **377**, 389 (2003).
7. Frontera, F., Zdziarski, A. A., Amati, L., Mikołajewska, J., Belloni, T., Del Sordo, S., Haardt, F., Kuulkers, E., Masetti, N., Orlandini, M., Palazzi, E., Parmar, A. N., Remillard, R. A., Santangelo, A., and Stella, L., *ApJ*, **561**, 1006 (2001).
8. Maccarone, T. J., and Coppi, P. S., *MNRAS*, **335**, 465 (2002).
9. Magdziarz, P., and Zdziarski, A. A., *MNRAS*, **273**, 837–848 (1995).
10. Zdziarski, A. A., Grove, J. E., Poutanen, J., Rao, A. R., and Vadawale, S. V., *ApJL*, **554**, L45 (2001).
11. White, T. R., Lightman, A. P., and Zdziarski, A. A., *ApJ*, **331**, 939 (1988).
12. Ballantyne, D. R., Vaughan, S., and Fabian, A. C., *MNRAS*, **342**, 239 (2003).
13. Zdziarski, A. A., Gierlinski, M., Mikołajewska, J., Wardziński, G., Harmon, B. A., and Kitamoto, S., *ArXiv*

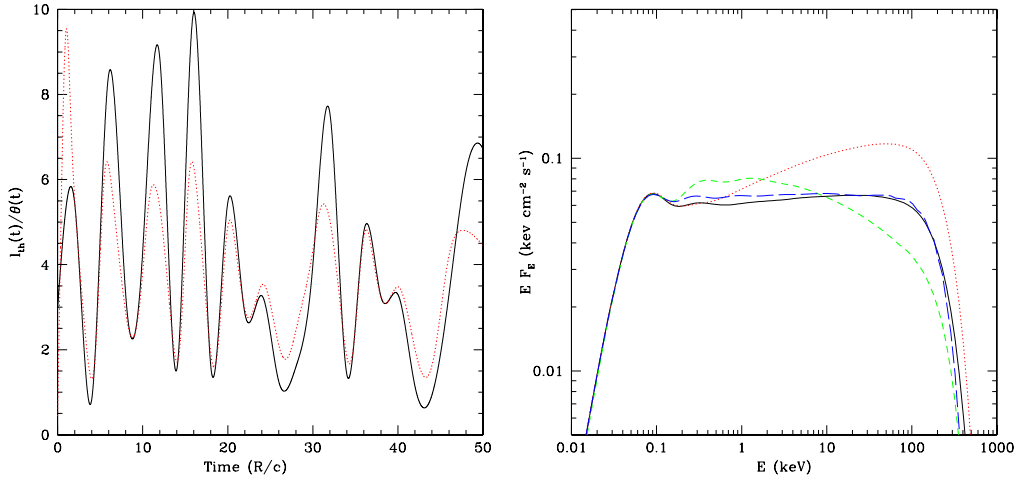


FIGURE 10. Comparison of a time-averaged thermal Comptonization spectrum with an equilibrium, steady-state Comptonization spectrum. The time-averaged spectrum was computed using a time-dependent, one-zone Comptonization code [31] while the steady state one was computed using EQPAIR. The seed photon density was kept constant while the electron heating rate, $l_{th}(t)$, varied as shown by the *solid* curve in the *left-hand* panel. The time-averaged value of the heating rate is $\langle l_{th}(t) \rangle = 4$. The corresponding time-response of the plasma's electron temperature, $\theta = kT_e/m_e c^2$, is shown by the *dotted* curve in the same panel. (The temperature values has been rescaled for clarity. The large temperature spike at $t \sim 0$ is due to the initial conditions.) The *solid* curve in the *right-hand* panel shows the time-averaged spectrum obtained by integrating the instantaneous escaping spectrum over time. The *short-dashed* and *dotted* curves in that panel show respectively the instantaneous escaping spectra at $t = 18$ (when $l_{th} = 1.6$, i.e., has a low value) and at $t = 31$ (when $l_{th} = 6.6$, i.e., a high value). For comparison, the *long-dashed* curve in that panel is the equilibrium spectrum computed assuming $l_s = 1$ and $l_{th} = \langle l_{th}(t) \rangle = 4$. While the instantaneous spectra are very different and in general are *not* well-fit by equilibrium spectra, note the good agreement between the time-averaged and equilibrium spectra.

- Astrophysics e-prints* (2004).
14. Pottschmidt, K., Wilms, J., Chernyakova, M., Nowak, M. A., Rodriguez, J., Zdziarski, A. A., Beckmann, V., Kretschmar, P., Gleissner, T., Pooley, G. G., Martínez-Núñez, S., Courvoisier, T. J.-L., Schönfelder, V., and Staubert, R., *A&A*, **411**, L383 (2003).
 15. Grove, J. E., "Gamma-Ray Observations of Galactic Black Hole Candidates," in *ASP Conf. Ser. 161: High Energy Processes in Accreting Black Holes*, 1999, p. 54.
 16. Laurent, P., and Titarchuk, L., *ApJ*, **511**, 289 (1999).
 17. Markoff, S., Nowak, M., Corbel, S. V., Fender, R., and Falcke, H., *New Astronomy Review*, **47**, 491 (2003).
 18. Jain, R. K., Bailyn, C. D., Orosz, J. A., McClintock, J. E., and Remillard, R. A., *ApJL*, **554**, L181 (2001).
 19. Nowak, M. A., Wilms, J., and Dove, J. B., *MNRAS*, **332**, 856 (2002).
 20. Maccarone, T. J., and Coppi, P. S., *MNRAS*, **338**, 189 (2003).
 21. Maitra, D., and Bailyn, C. D., *ArXiv Astrophysics e-prints* (2004).
 22. Poutanen, J., Krolik, J. H., and Ryde, F., *MNRAS*, **292**, L21 (1997).
 23. Esin, A. A., McClintock, J. E., and Narayan, R., *ApJ*, **489**, 865+ (1997).
 24. Poutanen, J., and Coppi, P. S., "Unification of Spectral States of Accreting Black Holes," in *Abstracts of the 19th Texas Symposium on Relativistic Astrophysics and Cosmology, held in Paris, France, Dec. 14-18, 1998*. Eds.: J. Paul, T. Montmerle, and E. Aubourg (CEA Saclay), 1998.
 25. Beloborodov, A. M., *ApJL*, **510**, L123 (1999).
 26. Zdziarski, A. A., Lubiński, P., Gilfanov, M., and Revnivtsev, M., *MNRAS*, **342**, 355–372 (2003).
 27. McConnell, M. L., Zdziarski, A. A., Bennett, K., Bloemen, H., Collmar, W., Hermsen, W., Kuiper, L., Paciesas, W., Philips, B. F., Poutanen, J., Ryan, J. M., Schönfelder, V., Steinle, H., and Strong, A. W., *ApJ*, **572**, 984 (2002).
 28. Sobczak, G. J., McClintock, J. E., Remillard, R. A., Cui, W., Levine, A. M., Morgan, E. H., Orosz, J. A., and Bailyn, C. D., *ApJ*, **544**, 993 (2000).
 29. Kubota, A., and Makishima, K., *ApJ*, **601**, 428 (2004).
 30. Kazanas, D., Hua, X., and Titarchuk, L., *ApJ*, **480**, 735 (1997).
 31. Coppi, P. S., *MNRAS*, **258**, 657 (1992).
 32. Maccarone, T. J., Coppi, P. S., and Poutanen, J., *ApJL*, **537**, L107 (2000).
 33. Gilfanov, M., Churazov, E., and Revnivtsev, M., *MNRAS*, **316**, 923 (2000).
 34. Poutanen, J., *MNRAS*, **332**, 257 (2002).